Resonant multilead point-contact tunneling

Chetan Nayak and Matthew P. A. Fisher
Institute for Theoretical Physics, University of California, Santa Barbara, California 93106-4030

A. W. W. Ludwig
Institute for Theoretical Physics, University of California, Santa Barbara, California 93106-4030
and Physics Department, University of California, Santa Barbara, California 93106-4030

H. H. Lin
Physics Department, University of California, Santa Barbara, California 93106-4030
(Received 16 December 1997)

We analyze a model of resonant point-contact tunneling between multiple Luttinger-liquid leads. The model is a variant of the multichannel Kondo model and can be related to the quantum Brownian motion of a particle on lattices with π flux through each plaquette (in the three-lead case, it is a honeycomb lattice with π flux). By comparing the perturbative and instanton gas expansions, we find a duality property of the model. At the boundary, this duality exchanges Neumann and Dirichlet boundary conditions on the Tomonaga-Luttinger bosons, which describe the leads; in the bulk, it exchanges the ''momentum'' and ''winding'' modes of these bosons. Over a certain range of Luttinger-liquid parameter g, a nontrivial intermediate coupling fixed-point controls the low-energy physics. The finite conductance at this fixed point can be exactly computed for two special values of g. For larger values of g, there is a stable fixed point at strong coupling that has enhanced conductance resulting from an analogue of Andreev reflection at the point contact. [S0163-1829(99)06023-3]

I. INTRODUCTION

Despite being a subject of intense interest in recent years, the study of strongly correlated electron systems has had a checkered history, primarily for two reasons. On the one hand, nonperturbative techniques— of which there are precious few—are required for their analysis. At the same time, these systems often exhibit unexpected phenomena, rendering useless our intuition culled from Fermi-liquid theory and other essentially perturbative problems. The greatest progress has been made on one-dimensional systems and, particularly, quantum impurity problems. In this arena, powerful techniques such as conformal field theory[1] and the Bethe ansatz,[2,3] have led to the discovery of a number of unusual properties (including spin-charge separation) which are fundamentally nonperturbative.

In this paper, we analyze a quantum impurity model that can be physically realized in a resonant tunneling junction between multiple quantum wires or quantum Hall edges. Our interest in this problem is threefold. First, the results we find—both intermediate-coupling fixed points and enhanced conductance due to an analogue of Andreev reflection at strongcoupling—are interesting in and of themselves because they truly are, to use a cliche, exotic. Second, both the methods used and the result may shed light on some of the recurrent themes in the study of correlated electron systems in which a single-particle picture is not valid. In particular, we demonstrate a highly nontrivial duality that exchanges strong and weak coupling. Recent progress in supersymmetric field theory and string theory hints at the possibility that such strong-weak coupling dualties are a common, perhaps even generic, feature of stongly coupled field theories. The duality discussed in this paper has a very rich structure and is one of the best examples of such a duality in a strongly correlated electron system. Finally, this model appears to be more generic and less fine-tuned than many similar ones, which leads us to hope that our findings could have consequences for future measurements.

In the next section, we formulate a model describing several Luttinger-liquid leads. Electrons can tunnel at a point contact from one of the Luttinger liquids to a resonant state (e.g., a quantum dot or island); from the resonant state, they can then proceed and tunnel to another of the Luttinger-liquid leads. A renormalization-group analysis shows that when the Luttinger-liquid parameter g is greater than 1/3, the tunneling process is relevant. In Sec. III, following,[4–6] we go to a limit in which we can make an instanton gas expansion of the strong-coupling limit;[7] an examination of this limit suggests a strong-weak coupling duality. This duality leads us to propose the phase diagram of Fig. 4. There are three interesting points in this phase diagram at which we can extract a more detailed understanding of the physics of this model. At $g=1$, the electrons in the leads are noninteracting. If we assume that there is no interaction between the electrons at the ends of the leads and an electron on the resonant state, then the problem is a free fermion problem, and can be solved exactly; the solution is discussed in Sec. IV. If, however, we assume that there is such an interaction, as we do for $g\neq 1$, a different fixed point results. (We need such an interaction in order to pass to the Toulouse limit, as we discuss below. The $g=1$ model can be continuously deformed into the $g\neq 1$ models only when this interaction is nonvanishing.) We make a conjecture about the relationship between these fixed points. At $g=\sqrt{3}$, the model is self-dual; this property allows us to deduce the conductance. Finally, for $g>9$, the strong-coupling fixed point is stable. At this fixed point, as we explain in Sec. V, we find an analog of Andreev reflection, which leads to enhanced conductance,

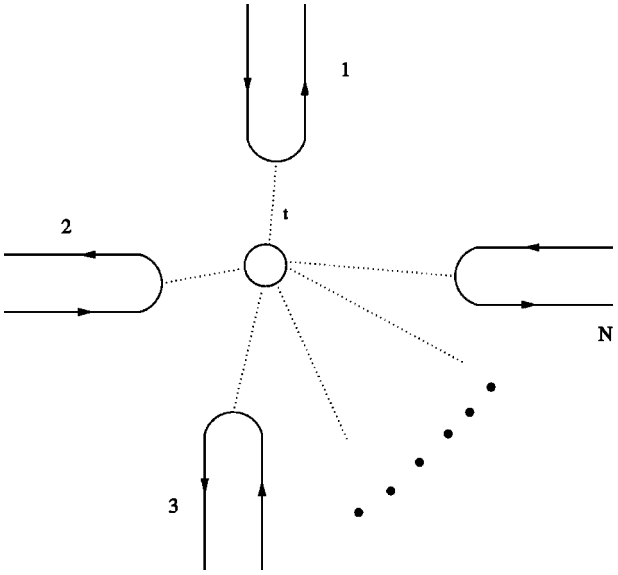

FIG. 1. A multilead resonant tunneling setup.

$G>g$. We also compute charge-transfer selection rules that elucidate the nature of this fixed point. We emphasize throughout the place of this model within the general framework of boundary conformal field theory and describe the most unusual features—namely, the duality and the Andreev processes—from several different points of view.

II. THE MODEL

A. The model and formalism

We consider a model in which N leads are coupled to each other through a resonant state, as in Fig. 1. One possible realization of this model is a quantum Hall bar in which quasiparticles or electrons can tunnel between several edges by first hopping from one edge to a dot or antidot and then hopping from there to another edge. An alternative implementation of this model is a resonant tunneling junction between N quantum wires. The former is more naturally described[8] by the ''*unfolded*'' formalism of Fig. 2(a) in which the leads are described by *chiral* bosons on an *infinite* line:

$$S_0=\int_{-\infty}^{\infty}dx\int d\tau\frac{g}{4\pi}\partial_x\phi_i(\partial_\tau+v\partial_x)\phi_i\,. \qquad (2.1)$$

τ is the imaginary time, and g and v are, respectively, the Luttinger paramater and velocity of the bosons, which we take, without loss of generality, to be the same in all leads. The chiral boson ϕ_i is an angular variable, $\phi_i\equiv\phi_i+2\pi$.

The quantum wire problem is more naturally expressed in terms of a nonchiral Luttinger liquid. This can be visualized in terms of the ''*folded*'' setup[3,9,10] of Fig. 2(b), in which the lead is modeled by a *nonchiral* Luttinger liquid on the *halfline* $x<0$:

$$S_0=\int_{-\infty}^{0}dx\int d\tau\ \frac{1}{8\pi}[(\partial_\tau\varphi_i)^2+v^2(\partial_x\varphi_i)^2]. \qquad (2.2)$$

[The two models are not quite equivalent since in a quantum wire or any other nonchiral Luttinger liquid, the electron

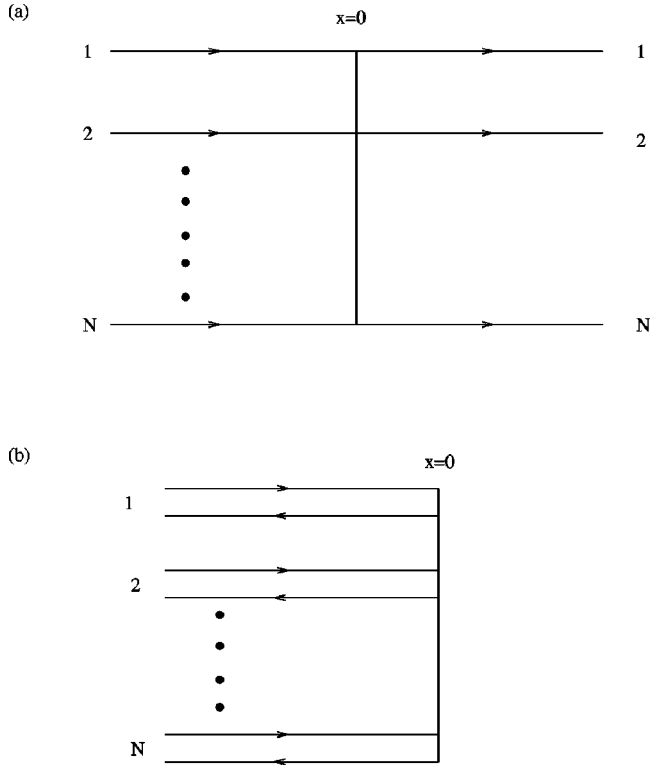

FIG. 2. The physical picture in the (a) ''unfolded'' formalism and (b) ''folded'' formalism.

creation operator has spin (i.e., $h-\bar{h}$) 1/2 and scaling dimension $1/2g$ (i.e., $h+\bar{h}$) while the electron creation operator in a chiral Luttinger liquid (2.1) is a dimension-$1/2g$, spin-$1/2g$ operator. The two models can be mapped into each other by a transformation that mixes left- and right-moving modes, but point-contact tunneling is insensitive to this mixing, so all of our results apply equally to both the ''folded'' and ''unfolded'' model.]

The fields φ_i are taken to be angular variables satisfying the periodicity condition $\varphi_i\equiv\varphi_i+2\pi(2\sqrt{g})$ (see Appendix C). (The quantity g is related to the usual compactification radius r of the bosonic string[11] via $r=2\sqrt{g}$.) In terms of chiral fields, $\varphi_i=\varphi_{iR}+\varphi_{iL}$. By this ''folding'' procedure, we have mapped $\phi(x>0)$ to φ_L, as depicted in Fig. 2. We will use both the folded and unfolded languages as convenient. Throughout this paper, we use ϕ_i for *unfolded*, and φ_i for *folded* bosons.

The term that transfers charge to the resonant level is (in the ''unfolded'' formalism, the corresponding term is the same, but with $\varphi_i/2\sqrt{g}$ replaced by ϕ):

$$S_t=t\int d\tau\sum_j\ (\eta_jS^+e^{-i\varphi_j(0)/2\sqrt{g}}+\eta_jS^-e^{i\varphi_j(0)/2\sqrt{g}}). \qquad (2.3)$$

Here, we have replaced the charge state of the resonant level by a spin-1/2 degree of freedom. The spin raising and lowering operators $S^{\pm}$ are the creation and annihilation operators for an electron or quasiparticle on the resonant level. The cocycles η_i must anticommute,

$$\{\eta_i,\eta_j\}=2\delta_{ij}\,, \qquad (2.4)$$

so that the tunneling operators have the correct bosonic commutation relations. This is true even when Eq. (2.3) transfers anyonic quasiparticles between the leads, so this model at $g=3$ describes tunneling between quantum Hall edges via an antidot in the interior of a Hall droplet at $\nu=1/3$. (See Appendix A.) In this paper, we focus in detail on $N=3$. In this case, the η_i's can be represented by Pauli matrices. In general, the η_i's are determined by the condition (2.4). When the leads are decoupled ($t=0$), the fields φ_i have Neumann boundary conditions at $x=0$; for $t\neq 0$, some other conformally invariant boundary condition is dynamically generated in the infrared.

Here, we are assuming that the level is perfectly resonant and that the different leads are coupled to this level with the same hopping strength t. In an experiment, the resonance can be tuned by controlling one parameter, such as a backgate voltage. If there are three leads (the simplest case with a nontrivial phase diagram), then two more parameters must be tuned to ensure that the hopping strengths are equal.

The fields ϕ_i, φ_i can be interpreted in terms of the voltage drops along and between leads.[12] In the ''unfolded'' formalism, the field ϕ_i can be discontinuous across $x=0$, and this discontinuity, $\phi_i(0+)-\phi_i(0-)$, is proportional to the voltage drop across $x=0$ in the ith lead. When the leads are decoupled, there is no voltage drop along the ''unfolded'' leads, $\phi_i(0+)=\phi_i(0-)$ or, equivalently, $\varphi_R(0)=\varphi_L(0)$ (Neumann boundary condition; see Appendix C). On the other hand, the voltage drop between leads i and j at the contact is proportional to $\varphi_i(0)-\varphi_j(0)$. In most of the following, we will use the ''folded'' formalism, but all of our results can be reinterpreted in the other language. In Appendix C, we discuss the conventions for these bosonic fields φ_i. In particular, we discuss the mode expansions of these fields and the zero modes, which play a crucial role in the following analysis. In terms of the ''momentum'' zero modes (see Appendix C), the Neumann boundary conditions have the effect of reflecting the zero modes of incoming states into those of outgoing states, $P_L^i=P_R^i$. When $t\neq 0$, these momenta are instead shifted, $P_L^i=P_R^i+Q^i$. The allowed shifts Q^i lie on a lattice that is connected to the problem of quantum Brownian motion in a periodic potential, as we will discuss in the next section.

First, however, we note that the Kubo formula for the conductance (obtained in the usual way, see, e.g., Ref. 4, by introducing a vector potential A between the resonant level and one of the leads, say lead three, and differentiating the partition function with respect to A) takes the following form:

$$G=2g\left[1-\frac{|\omega|}{2\pi}\langle\varphi_3(x=0,\omega)\varphi_3(x=0,-\omega)\rangle\right]. \quad (2.5)$$

When $t=0$, φ_3 is a free field with Neumann boundary condition at $x=0$, so $|\omega|\langle\varphi_3(x=0,\omega)\varphi_3(x=0,\omega)\rangle=2\pi$ and therefore, $G=0$, as we would expect since the leads are decoupled.

B. The Toulouse limit and quantum Brownian motion

Let us focus, for the moment, on the case $N=3$. The case of general N can be worked out in an analogous fashion, but we choose not to give details here. We rewrite Eqs. (2.1) and (2.3) as

$$S=\int_{-\infty}^{0}dx\int d\tau\frac{1}{8\pi}\partial_\mu\varphi_i\partial^\mu\varphi_i + t\,\delta(x)\sum_j\left(\eta_j S^+ e^{-i(\mathbf{R}_\parallel^j\cdot\boldsymbol{\varphi}+\mathbf{R}_\perp\cdot\boldsymbol{\varphi})}+\eta_j S^- e^{i(\mathbf{R}_\parallel^j\cdot\boldsymbol{\varphi}+\mathbf{R}_\perp\cdot\boldsymbol{\varphi})}\right) \quad (2.6)$$

where $\boldsymbol{\varphi}=(\varphi_1,\varphi_2,\varphi_3)$ and $\mathbf{R}_\parallel^1=(1/6\sqrt{g})(2,-1,-1)$, $\mathbf{R}_\parallel^2=(1/6\sqrt{g})(-1,2,-1)$, $\mathbf{R}_\parallel^3=(1/6\sqrt{g})(-1,-1,2)$, and $\mathbf{R}_\perp=(1/3\sqrt{2g})(1,1,1)$. With this notation, we have anticipated the mapping to the problem of quantum Brownian motion on a honeycomb lattice with lattice vectors $\mathbf{R}_\parallel^1$, $\mathbf{R}_\parallel^2$, $\mathbf{R}_\parallel^3$, and S_z keeping track of the sublattice. There is one step left before such an identification can be complete, namely, decoupling $\mathbf{R}_\perp\cdot\boldsymbol{\varphi}$ by going to the Toulouse limit as in Refs. 5 and 6. To do this, we modify the Hamiltonian related to Eq. (2.6) by

$$\mathcal{H}\rightarrow\mathcal{H}+\tilde{t}_z\delta(x)\left(\sum_i\Pi_i\right)S_z\Big/2\sqrt{g}, \quad (2.7)$$

where Π is the momentum conjugate to $\boldsymbol{\varphi}$. The added term is an interaction between the charge of the resonant level and the charge density of the lead at the point contact. As a result of this term, the modified Lagrangian describes an interacting system even at $g=1$ although in this case the interaction takes place only at $x=0$. Such a term is not forbidden by any symmetry of the model and is known not to affect the low-energy physics in the multichannel Kondo problem. We will assume that Eq. (2.6) and the modified Lagrangian flow to the same infrared fixed point and restrict our attention to Eq. (2.7) from now on. This assumption does not appear to be valid at $g=1$, which might be special to $g=1$, as we discuss in Sec. IV. The advantage of adding such a term to the Lagrangian is that we can now[5,6] perform a canonical transformation generated by $U=e^{i\tilde{t}_z\Sigma_i\varphi_i(0)S_z/2\sqrt{g}}$. (To be more rigorous, we should use $U=e^{i\tilde{t}_z\Sigma_i\varphi_i(0)S_z/2\sqrt{g}}e^{-i\tilde{t}_z\Sigma_i\varphi_i(-\infty)\,S_z/2\sqrt{g}}$, which is overall charge neutral since only integer charges can be added to the systen. The second exponential compensates the fractional charge added at 0 by removing an equal amount at $-\infty$.) This has the effect of simultaneously removing the term, which we just added and removing the $\mathbf{R}_\perp\cdot\boldsymbol{\varphi}$ terms from the exponentials in the tunneling Lagrangian if we choose $\tilde{t}_z=1/N$. This leaves us, finally, with the Lagrangian

$$S=\frac{1}{8\pi}\partial_\mu k_i\partial^\mu k_i+t\,\delta(x)\sum_j\left(\eta_j S^+ e^{-i\mathbf{R}^j\cdot\mathbf{k}}+\eta_j S^- e^{i\mathbf{R}^j\cdot\mathbf{k}}\right), \quad (2.8)$$

where

$$\mathbf{k}=(k_x,k_y,k_z)=\left(\frac{1}{\sqrt{2}}(-\varphi_1+\varphi_2),\frac{1}{\sqrt{6}}(-\varphi_1-\varphi_2+2\varphi_3),\frac{1}{\sqrt{3}}(\varphi_1+\varphi_2+\varphi_3)\right) \quad (2.9)$$

and

$$\mathbf{R}^1=\sqrt{\frac{1}{3g}}(-\sqrt{3}/2,-1/2,0),$$

$$\mathbf{R}^2=\sqrt{\frac{1}{3g}}(\sqrt{3}/2,-1/2,0), \tag{2.10}$$

$$\mathbf{R}^3=\sqrt{\frac{1}{3g}}(0,1,0).$$

∂k_x and ∂k_y are the Cartan generators of an SU(3) that ''rotate'' the leads (which is a symmetry of the free Lagrangian at certain special points such as $g=1,1/2$). Yi and Kane[6] showed that the three-channel Kondo problem is one of a class of models (namely, the $g=1/2$ point) which may be formulated as the quantum Brownian motion of a particle on a honeycomb lattice. In Eq. (2.8), we have almost the same problem. The crucial difference is the presence of the η_i's, which results in a π flux through each plaquette of the honeycomb lattice. This may be seen by considering the amplitude for a circuit around a plaquette, which involves the product $\eta_1\eta_2\eta_3\eta_1\eta_2\eta_3=-1$.

The RG equation for t may be obtained from the scaling dimension of the field $e^{i\mathbf{R}^i\cdot\mathbf{k}}$, which is $|\mathbf{R}^i|^2=1/3g$:

$$\frac{dt}{dl}=\left(1-\frac{1}{3g}\right)t+\cdots. \tag{2.11}$$

Hence, for $g<1/3$, t flows to zero in the infrared and the leads are decoupled. For $g>1/3$, t grows with decreasing energy scales. The upshot of this growth will be analyzed in the next section using a duality property of this model.

The partition function may be expanded perturbatively in powers of t

$$Z=\sum_n\sum_{\{l_j\}}\frac{t^n}{n!}\int d\tau_1\cdots d\tau_n\delta\left(\sum_j \epsilon_j\mathbf{R}^{l_j}\right)\times\exp\left(\sum_{i>j}\epsilon_i\epsilon_j\mathbf{R}^{l_i}\cdot\mathbf{R}^{l_j}\ln|\tau_i-\tau_j|+i\pi\theta(\tau_i-\tau_j)\times(1-\delta_{l_il_j})\right) \tag{2.12}$$

$l_i=1,2,3$, $\epsilon_i=\pm1$, and the ϵ_i's must alternate chronologically. If we ignore the second term in the exponential, this is the partition function (at $g=1/2$) of the three-channel Kondo model. It is a two-component Coulomb gas. The second term gives a minus sign whenever the order of two unlike hops is exchanged, thereby implementing the π flux.

C. An auxiliary model

We will also consider a simpler model (which is discussed in Ref. 6) for the purposes of comparison with and illumination of the resonant tunneling model described above. This model can be analyzed without going to a Toulouse limit, and it exhibits Andreev reflection at a strong-coupling fixed point and a duality property with a straightforward interpretation. This instills us with more confidence that these properties of Eq. (2.8) are generic and are not particular to the Toulouse limit. It is defined by

$$S=\int_{-\infty}^{\infty}dx\int d\tau\frac{1}{4\pi}\partial_x\phi_i(\partial_\tau+i\partial_x)\phi_i+t\delta(x)\sum_{i\neq j=1,2,3}(e^{-i(\phi_i-\phi_j)/\sqrt{2g}}+e^{i(\phi_i-\phi_j)/\sqrt{2g}}). \tag{2.13}$$

This is a model of quantum Brownian motion on a triangular lattice. In fact, this is the same triangular lattice that is the underlying Bravais lattice of the above honeycomb lattice, as may be seen by writing the Lagrangian (2.13) as $(\partial_\mu\mathbf{k})^2+t\delta(x)\Sigma_j e^{\mathbf{k}\cdot\mathbf{R}^j}+\text{H.c.}$ with $\mathbf{k}$ as in Eq. (2.9) and $\mathbf{R}^j$ given by Eq. (2.10) with the first and second components interchanged. At $g=1$, Eq. (2.13) has a fermionic representation

$$S=\int_{-\infty}^{\infty}dx\int d\tau\psi_i^\dagger(\partial_\tau+i\partial_x)\psi_i+t\delta(x)\epsilon^{ijk}\eta_k\psi_i^\dagger\psi_j. \tag{2.14}$$

This is not a free fermion problem because the fermion interacts with a spin-1/2 degreee of freedom η_i which is present to give the correct commutation relations, as in Eq. (2.3). This model is actually a generalized multichannel Kondo model in which the conduction electrons transform in an SU(2) triplet. The infrared fixed point can be solved for exactly[13] in complete analogy with the methods employed in the ordinary multichannel Kondo model.[1] Interestingly, it is related to the ordinary four-channel, spin-1/2 Kondo fixed point. According to Ref. 6, the model flows to strong coupling at $g=1$. Hence, the fixed point of Ref. 13 is an example of the Andreev reflection phenomenon, which we discuss below. The advantage of this model lies in the fact that there are no complications related to the Toulouse limit, as there are in Eq. (2.8). It is particularly simple from the point of view of duality.

III. DUALITY

If $g>1/3$, t is a relevant coupling, so an initially small t grows in the infrared. When t is large, the interaction term, $t\delta(x)\Sigma_i(\eta_jS^+e^{-i\mathbf{R}^i\cdot\mathbf{k}}+\eta_jS^-e^{i\mathbf{R}^i\cdot\mathbf{k}})$ will be dominant and, in a semiclassical analysis, k will be localized at one of its minima. These minima are just the minima of the energy bands of a particle on a tight-binding honeycomb lattice with π flux per plaquette. There are four such energy bands since the π flux doubles the unit cell and since the honeycomb lattice, to begin with, is a triangular lattice with a two site basis. (We represent η_j by Pauli matrices τ_j.) They correspond to the four possible S_z and τ_3 quantum numbers. At low energies, k will be in one of the minima of the lowest band. These also form a honeycomb lattice; the lattice displacements—i.e., the analogs of the $\mathbf{R}^i$'s—on this honeycomb lattice are

$$\mathbf{K}^1=\frac{\sqrt{g}}{3}(0,1),$$

$$\mathbf{K}^2=\frac{\sqrt{g}}{3}(\sqrt{3}/2,-1/2), \tag{3.1}$$

$$\mathbf{K}^3=\frac{\sqrt{g}}{3}(-\sqrt{3}/2,-1/2).$$

The partition function can be approximated by an instanton gas in which the instantons are solutions of the Euclidean equations of motion in which k tunnels between different minima. As usual in this class of problem,[7] the instanton gas expansion can be formulated as a Coulomb gas. There is an additional subtlety here, however: there is a Berry's phase associated with the instanton solutions. Details will be given in an appendix; here we merely sketch the derivation. Note that the minima of the lowest band surround a point at which the two lowest bands touch. The Berry's phase will be the same for any path surrounding this point, so we consider a path that is very close to this point. For such paths, $\Sigma_j(\eta_j S^+ e^{-i\mathbf{R}^j\cdot\mathbf{k}}+\eta_j S^- e^{i\mathbf{R}^j\cdot\mathbf{k}})$ can essentially be approximated by $-\delta k_x\sigma_z-\delta k_y\sigma_x$. Here, the four energy bands, acted on by $\eta\otimes S$, are reduced to the two-dimensional subspace of the two lowest bands, acted on by the σ's. δk_x, δk_y are k_x, k_y measured from the contact point of the two bands. As $\delta\mathbf{k}$ traces out a path around 0, the spin σ rotates by 2π and therefore accrues a Berry phase of π. Hence, the Coulomb gas defined by the instanton expansion is a Coulomb gas with phases. In fact, it is of precisely the same variety as that defined by the perturbative expansion of Eq. (2.8). More concretely, the instanton—or strong-coupling—expansion of Eq. (2.8) is equal to the perturbative—or weak-coupling—expansion of

$$\mathcal{L}_{Dual}=\int_{-\infty}^{0}dx\int d\tau\frac{1}{8\pi}\partial_\mu r_i\partial^\mu r_i+v\,\delta(x)$$

$$\times\sum_j(\eta_j S^+ e^{-i\mathbf{K}^j\cdot\mathbf{r}}+\eta_j S^- e^{i\mathbf{K}^j\cdot\mathbf{r}}). \tag{3.2}$$

[Here r_i is the field dual to the field k_i of Eq. (2.9) in the usual way, as reviewed in Appendix C.] The $v\to 0$ limit of Eq. (3.2) is equivalent to the $t\to\infty$ limit of Eq. (2.8) and, conversely, the $v\to\infty$ limit is equivalent to the $t\to 0$ limit. In effect, the duality exchanges $g\to 3/g$. For small v, we can obtain the RG equation for v just as we did for t above

$$\frac{dv}{dl}=\left(1-\frac{g}{9}\right)v+\cdots. \tag{3.3}$$

Combining Eqs. (2.11) and (3.3), we find that the $t=0$ limit is stable for $g<1/3$ while the $t=\infty$ limit is stable for $g>9$. In the former, weak-coupling limit, the fields k_x,k_y have Neumann boundary conditions at $x=0$, while r_x, r_y have Dirichlet boundary conditions. In the latter, strong-coupling limit, k_x,k_y satisfy Dirichlet boundary conditions at $x=0$, while r_x,r_y have Neumann boundary conditions. Since k_z decouples, it always has Neumann boundary conditions and consequently r_z always has Dirichlet boundary conditions. For $1/3<g<9$, both limits are unstable and we expect a stable fixed point at intermediate coupling or, in other words, a nontrivial conformally invariant boundary condition. The situation is summarized by Fig. 2. There are two intermediate coupling fixed points at which we can calculate the conductance exactly

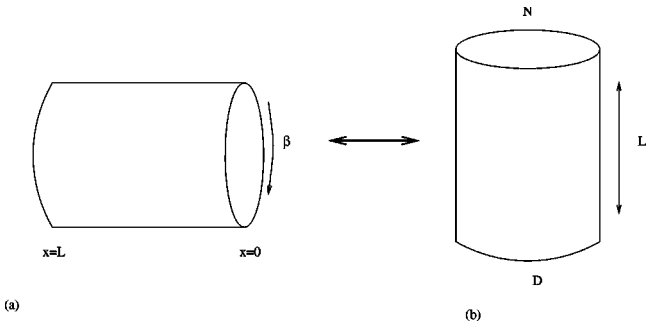

FIG. 3. The (a) finite-temperature partition function of this model can be represented as (b) the closed string amplitude for propagation between boundary states D and N.

(a) At $g=1$, where a free fermion formulation is available for $\tilde{t}_z=0$. We do not believe that the $\tilde{t}_z=0$ model has the same physics as the $\tilde{t}_z=1/N$ model, but it is instructive to compare the two cases.

(b) At $g=\sqrt{3}$, the model is self-dual. It may be shown[7] that the duality exchanges

$$(|\omega|/2\pi)\langle k_x k_x\rangle\to 1-(|\omega|/2\pi)\langle r_x r_x\rangle$$

(and the same for k_y) as we discuss in an appendix. At the self-dual point, $\langle k_x k_x\rangle=\langle r_x r_x\rangle$, so $G=g(2/3)=2/\sqrt{3}$.

We will also discuss at length the conductance at (c) the strong-coupling fixed point, which is stable for $g>9$.

First, however, we will make a few more comments on the duality between Eqs. (2.8) and (3.2). One point that should be emphasized is that the duality is only approximate. It is strictly a duality between the instanton gas expansion of Eq. (2.8) and the perturbative expansion of Eq. (3.2) (and vice versa). In the asymptotic low-energy limit, the instanton gas expansion of Eq. (2.8) is the dominant contribution to the partition function when t is large, but at finite energy there are corrections. If we were to attempt to formulate an exact duality, these corrections would be manifested by the presence of a presumably infinite number of additional irrelevant terms in Eq. (3.2).[3]

The perturbative expansion of Eq. (2.8) is an expansion in current-generating charge-transfer events while the instanton gas is an expansion in voltage-generating phase slips [in Eq. (3.2), the roles are reversed]. This formulation of the duality concentrates on the values of the fields at the point contact. A related but alternative way of understanding this duality arises from the natural notion of duality inherent in the bulk (i.e., the duality of closed strings with toroidal compactification). Let us first look at the simpler model Eq. (2.13). Following the same steps that led to Eq. (3.2), we see that Eq. (2.13) is dual to a theory described by the same Lagrangian (2.13), but with the replacement $g\to 3/4g$.[6] Let us consider the finite temperature partition function of this model in a finite-size system of length L, with Neumann boundary condition at $x=L$ and the interaction at $x=0$, as in Fig. 3(a).

This partition function can also be viewed (by turning it on its side) as the closed string amplitude for propagation between the dynamical boundary state at $x=0$ and the Neumann boundary state at $x=L$, as in Fig. 3(b). The closed string states are specified by their momenta, winding numbers, and oscillator mode occupancies (see Appendix C for a brief summary). The allowed momenta $\mathbf{P}$ for the fields $\mathbf{k}=[(1/\sqrt{2})(-\varphi_1+\varphi_2),(1/\sqrt{6})(-\varphi_1-\varphi_2+2\varphi_3)]$ are determined by the condition that the operator $e^{i\mathbf{P}\cdot\mathbf{k}}$ be well defined under the identification $\varphi_i\equiv\varphi_i+2\pi\sqrt{2g}$; the momenta form a triangular lattice with lattice constant $\sqrt{1/g}$. [As usual, we ignore $k_z=(1/\sqrt{3})(\varphi_1+\varphi_2+\varphi_3)$, which decouples.] The winding numbers $\mathbf{W}$ are the set of identifications, $\mathbf{k}\equiv\mathbf{k}+\mathbf{W}$; they form a triangular lattice with lattice constant $2\sqrt{g/3}$. There are two dual descriptions that result from exchanging the momenta and winding modes. This is precisely the same duality between triangular lattices, which exchanges the strong- and weak-coupling limits of Eq. (2.13). The model (2.8) can be embedded within this picture. The only additional structure is that the displacements on the triangular lattice (i.e., charge transfers or phase slips) are split into pairs of displacements on the honeycomb lattice in both the original and dual theories. Yet another interpretation in terms of S-matrix selection rules will be dicussed in the context of the Dirichlet boundary condition.[14]

IV. SOLUTION AT $g=1$

At $g=1$, the model defined by Eqs. (2.1) and (2.3) has the free fermion representation (in particular, with $\tilde{t}_z=0$)

$$\mathcal{L}=\int_{-\infty}^{\infty}dx\int d\tau\psi_i^\dagger(\partial_\tau+i\partial_x)\psi_i+d^\dagger\partial_\tau d+t\,\delta(x)\sum_i\psi_i^\dagger d+\psi_i d^\dagger. \tag{4.1}$$

The creation and annihilation operators of charge on the resonant state are denoted by $d^\dagger$, d rather than $S^\pm$, and $\{d,\psi\}=\{d,\psi^\dagger\}=0$, $\{d,d^\dagger\}=1$. This free fermion problem can be solved exactly. The equations of motion for ψ and d are

$$\partial_\tau\psi_i(x)=\partial_x\psi_i(x)+td\,\delta(x),\quad \partial_\tau d=t\sum_i\psi_i(0). \tag{4.2}$$

Integrating the first equation between $x=-\epsilon$ and $x=\epsilon$ and Fourier transforming, we find

$$\psi_i(\omega,0+)-\psi_i(\omega,0-)=-itd(\omega),\quad \omega d(\omega)=t\sum_i\psi_i(\omega). \tag{4.3}$$

In the second equation, $\psi_i=[\psi_i(0+)+\psi_i(0-)]/2$. From these $N+1$ equations, we can extract $\psi_i(\omega,0+)$ and $d(\omega)$ in terms of $\psi_i(\omega,0-)$. The solution may be summarized by the S matrix, $\psi_i(\omega,0+)=S_{ij}\psi_j(\omega,0-)$, where

$$S_{ii}=\frac{N-2}{N},\quad S_{ij}=\frac{-2}{N}\quad\text{for}\quad i\neq j. \tag{4.4}$$

The resulting conductance is

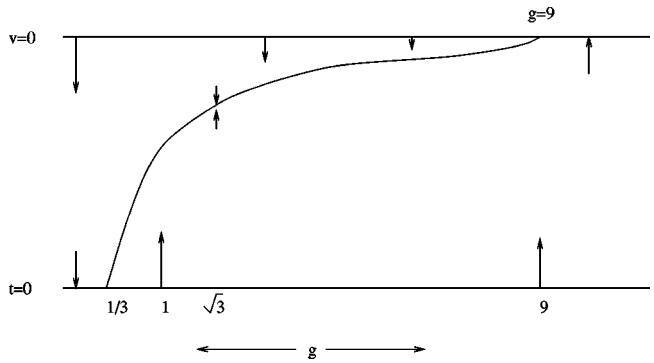

FIG. 4. The phase diagram. The horizontal axis measures g, the Luttinger-liquid parameter, and the vertical axis measures t, the hopping strength, and its dual variable v. The RG flows are as indicated. The intermediate coupling fixed points which are stable for $1/3<g<9$ are represented by the curve connecting the weak- and strong-coupling fixed points at $g=1/3$ and $g=9$, respectively.

$$G_{\text{free fermion}}=(N-1)\left(\frac{2}{N}\right)^2, \tag{4.5}$$

which, for 3 leads is $G=8/9$. It is somehwat remarkable that a free fermion problem could be an interediate-coupling fixed point with a nontrivial conductance. However, this is the maximal possible conductance consistent with unitarity and permutation symmetry for a three-lead free fermion problem. In other words, if we assume that

$$S_{ii}=r,\quad S_{ij}=t\quad\text{for}\quad i\neq j. \tag{4.6}$$

then unitarity, $S_{ij}S^*_{kj}=\delta_{ik}$, imposes the constraint $|r|\geqslant 1/3$, and, hence, $G\leqslant 8/9$. In the next section, we will discuss even larger conductances and the physics behind them.

First, however, we will comment on the relationship between the $\tilde{t}_z=0$ and $\tilde{t}_z=1/N$ fixed points. We do not believe that they are the same for two reasons. First, we expect G/g to be nondecreasing as g is increased. While $G(g=1,\tilde{t}_z=0)<G(g=\sqrt{3},\tilde{t}_z=1/3)$, $G(g=1,\tilde{t}_z=0)>G(g=\sqrt{3},\tilde{t}_z=1/3)/\sqrt{3}$. Hence, we expect that $G(g=1,\tilde{t}_z=1/3)<G(g=\sqrt{3},\tilde{t}_z=1/3)/\sqrt{3}<G(g=1,\tilde{t}_z=0)$. An additional point for consideration is that a small $\tilde{t}_z$ is an irrelevant perturbation at the $\tilde{t}_z=0$ fixed point, as may be seen by direct calculation. Similarly, a small deviation of $\tilde{t}_z$ from 1/3 is irrelevant at the $\tilde{t}_z=1/3$ fixed point, as may be shown perturbatively for $g\to 1/3$; it is reasonable to assume that this is true even at $g=1$. Hence, it is plausible that the $\tilde{t}_z=0$ fixed point described above lies out of the plane of the phase diagram of Fig. 4 with an unstable fixed point separating it from the $\tilde{t}_z=1/3$ fixed point.

V. DIRICHLET BOUNDARY CONDITIONS AND ANDREEV REFLECTION

A remarkable feature of this model reveals itself when we consider the conductance at the $t=\infty$ fixed point, which is stable for $g>9$ [and for $g>1$ in the auxiliary model (2.13)]. At this fixed point, $k_x=(1/\sqrt{2})(-\varphi_1+\varphi_2)$ and $k_y=(1/\sqrt{6})(-\varphi_1-\varphi_2+2\varphi_3)$ have Dirichlet boundary condi-

tions at $x=0$, while $k_3=(1/\sqrt{3})(\varphi_1+\varphi_2+\varphi_3)$ has Neumann boundary condition. As a result,

$$\frac{|\omega|}{2\pi}\langle\varphi_3(x=0,\omega)\varphi_3(x=0,\omega)\rangle=\frac{2}{3}\frac{|\omega|}{2\pi}\langle k_x(0,\omega)k_x(0,\omega)\rangle + \frac{1}{3}\frac{|\omega|}{2\pi}\langle k_3(0,\omega)k_3(0,\omega)\rangle = \frac{2}{3}(0)+\frac{1}{3}(1)=\frac{1}{3}, \tag{5.1}$$

where the second equality follows from the respective Dirichlet and Neumann boundary conditions of k_x and k_3. Hence, from Eq. (2.5) we have

$$G_3^{\max}=\frac{4}{3}g. \tag{5.2}$$

This is an astonishing result, since it implies that the conductance is greater than ''perfect'' conductance, $G=g$. [The scrupulous reader might worry that this surprising finding is due entirely to the Toulouse limit and is therefore incorrect. However, since the same conductance is found for Eq. (2.13) (which does not involve a Toulouse limit) at its strong-coupling fixed point, we believe that this result is robust.] We interpret this as the signature of *Andreev reflection*: the conductance is greater than its naive maximum value because a hole is backscattered at the point contact. Before pursuing this point further, let us note that for general N, the corresponding formula for the conductance at the strong-coupling fixed point is

$$G_N^{\max}=g\left(2-\frac{2}{N}\right). \tag{5.3}$$

For $N=2$, the maximum conductance is $G=g$, the naive value. For $N>2$, the maximum conductance is greater than this value, saturating at $G=2g$ in the $N\to\infty$ limit.

Why do we say that the enhanced conductance is due to Andreev reflection? In Eq. (2.5), $2-2(|\omega|/2\pi)\langle\varphi_3\varphi_3\rangle$ is, essentially, the transmitted fraction of the incoming current; $2(|\omega|/2\pi)\langle\varphi_3\varphi_3\rangle-1$ is the reflected fraction. At $g=1$, where the leads have a free fermion description, transmission t and reflection r coefficients can be defined;

$$2(|\omega|/2\pi)\langle\varphi_3\varphi_3\rangle-1=|r|^2.$$

By charge conservation we also have $(N-1)|t|^2+|r|^2=1$. $G>g$ precisely because the reflection coefficient is *negative*. In other words, the reflected current is a *negative* fraction of the incoming current—i.e., it is a current of holes rather than electrons.

Physically, the Dirichlet boundary condition corresponds to the limit in which there is no voltage difference between the different leads. For $N-1>1$ only a fraction of the current that leaves one lead enters any one of the other $N-1$ leads. Without Andreev scattering, this would lead to a voltage drop between the leads, but Andreev processes offset this voltage. An alternative perspective on the multichannel Dirichlet boundary condition is reminiscent of the situation explored in Ref. 14. Suppose we view $N-1$ of the leads as a single, aggregate lead described by a single charge boson with $g_{aggr}=g(N-1)$. Then, tunneling between the remaining lead and the aggregate lead is precisely the problem of tunneling between dissimilar Luttinger liquids considered in Ref. 14. This problem can be transformed to one with two identical Luttinger liquids with $1/g_{eff}=(1/g+1/g_{aggr})/2=N/2(N-1)g$. For such a problem, it is not surprising that the maximal conductance is $G_{\max}=g_{eff}=2g(N-1)/N$.

Yet another means of characterizing the Dirichlet boundary condition is by S-matrix selection rules for soliton scattering at the junction. This can be most conveniently done in the *unfolded* formalism. We use tildes to designate the unfolded counterparts of the *folded* fields k_i and their duals r_i. Following Ref. 14, we obtain these by rewriting the chiral fields ϕ_1, ϕ_2, ϕ_3 in terms of the dual fields $\tilde{r}_x$, $\tilde{r}_y$, which are free fields at the strong-coupling Dirichlet boundary condition fixed point. Working in the chiral (''unfolded'') notation, where $\tilde{k}_x=(\phi_1-\phi_2)/\sqrt{2}$, $\tilde{k}_y=(-\phi_1-\phi_2+2\phi_3)/\sqrt{6}$, we can define dual free fields $\tilde{r}_x$, $\tilde{r}_y$ via

$$\tilde{k}_x=\tilde{r}_x\theta(-x)-\tilde{r}_x\theta(x),\quad \tilde{k}_y=\tilde{r}_y\theta(-x)-\tilde{r}_y\theta(x). \tag{5.4}$$

This allows us to calculate the matrix elements

$$\left\langle \exp\left(-i\sum_j q_j^{\text{out}}\phi_j(x=\infty)/\sqrt{2g}\right)\times\exp\left(i\sum_j q_j^{\text{in}}\phi_j(x=-\infty)/\sqrt{2g}\right)\right\rangle. \tag{5.5}$$

The operators $e^{\mp iq_j^{\text{in,out}}\phi_j(\pm\infty)/\sqrt{2g}}$ create or destroy states with well-defined charges in the leads; the matrix elements (5.5) are proportional to the S-matrix elements between these different charge sectors. For generic $q_j^{\text{in,out}}$, Eq. (5.5) will vanish, which means that there is no scattering between these charge sectors in the strong-coupling (Dirichlet boundary condition) limit. Equation (5.5) will be nonvanishing only if the correlation function is charge neutral for each of the free fields $\tilde{r}_x$, $\tilde{r}_y$, $\tilde{k}_z$. Since these fields have Neumann boundary conditions, Eq. (5.4) has the following implications for Eq. (5.5):

$$q_1^{\text{in}}+q_2^{\text{in}}+q_3^{\text{in}}=q_1^{\text{out}}+q_2^{\text{out}}+q_3^{\text{out}},$$

$$q_1^{\text{in}}-q_2^{\text{in}}=-(q_1^{\text{out}}-q_2^{\text{out}}), \tag{5.6}$$

$$-q_1^{\text{in}}-q_2^{\text{in}}+2q_3^{\text{in}}=-(-q_1^{\text{out}}-q_2^{\text{out}}+2q_3^{\text{out}}).$$

Solving for the charges of the ''out'' states, one finds that the charge transfers lie on a honeycomb lattice,

$$\Delta\vec{q}\equiv\begin{pmatrix} q_1^{\rm in}\\ q_2^{\rm in}\\ q_3^{\rm in}\end{pmatrix}-\begin{pmatrix} q_1^{\rm out}\\ q_2^{\rm out}\\ q_3^{\rm out}\end{pmatrix}=\frac{2}{3}\left[\begin{pmatrix} 2\\ -1\\ -1\end{pmatrix}q_1^{\rm in}+\begin{pmatrix} -1\\ 2\\ -1\end{pmatrix}q_2^{\rm in}+\begin{pmatrix} -1\\ -1\\ 2\end{pmatrix}q_3^{\rm in}\right]. \tag{5.7}$$

Note that, for general ''in'' states, which carry in each lead multiples of the unit of charge, the charges of the ''out'' state in the individul leads are in general no longer multiples of the unit charge. This is a phenomenon analogous to the $N\geqslant 3$ flavor Callan-Rubakov effect.[15] In fact, the ''auxiliary model'' at $g=1$, discussed at the end of Sec. II, is an example where this situation occurs at an infrared fixed point for free electron leads. For example,

$$\langle e^{-i\phi_j(x=\infty)/\sqrt{2g}}e^{i\phi_1(-\infty)/\sqrt{2g}}\rangle=0 \tag{5.8}$$

for $j=1,2,3$. In other words, a unit of charge cannot be transferred from one lead to another or even reflected by the junction. On the other hand,

$$\langle e^{i\phi_1(x=\infty)/\sqrt{2g}}e^{-2i\phi_2(\infty)/\sqrt{2g}}e^{-2i\phi_3(\infty)/\sqrt{2g}}e^{3i\phi_1(-\infty)/\sqrt{2g}}\rangle\neq 0. \tag{5.9}$$

This is a clear illustration of the Andreev reflection property of the Dirichlet boundary condition for $N>2$. Three incoming electrons in lead 1 are scattered into two electrons into each of leads 2 and 3 and an Andreev reflected hole in lead 1.

ACKNOWLEDGMENTS

This work was supported in part by NSF Grant No. PHY94-07194 at ITP-UCSB. C.N. would like to thank C. de C. Chamon for discussions. C.N. and A.W.W.L. thank E. Fradkin for an explanation of his work. A.W.W.L. thanks the A.P. Sloan Foundation for financial support. M.P.A.F. is grateful to the National Science Foundation for support, under Grants Nos. PHY94-07194, DMR-9400142, and DMR-9528578.

APPENDIX A: COMMUTATION RELATIONS FOR THE KLEIN FACTORS

We need to introduce the all-important Klein factors η_i, because we would like to treat the fields φ_i as independent bosons that commute with each other. Since the underlying electron or quasiparticle operators are mutually fermionic or even anyonic, Klein factors must be introduced to compensate.

We begin with the commutation relations for the chiral version of the tunneling operators, $T_{ij}=e^{i\int_{x_j}^{x_i}\partial_x\phi}$, which are obtained from those of a single-chiral boson by imagining that the three-lead dot/antidot setup is deformed as in Fig. 5. As a result of the chiral boson commutations relations, the tunneling operators commute since they do not cross (see Fig. 5). This holds whether the objects which tunnel are fermions or anyons.

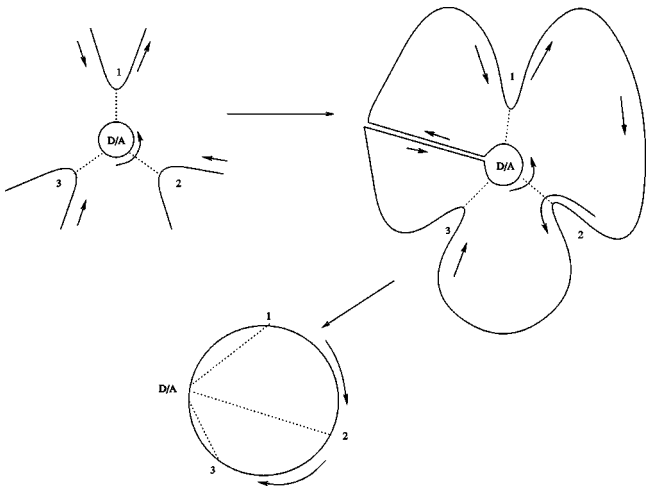

FIG. 5. Deformation of the resonant tunneling arrangement into a chiral boson on a circle.

In our model, we represent T_{ij} by $T_{ij}=\eta_j S^{\pm}e^{\mp i\phi_j}$ where η_j and $S^{\pm}$ commute with each other and with ϕ_j, and the ϕ_j's are mutually commuting. To ensure that the tunneling operators commute, we must take $\eta_i\eta_j=-\eta_j\eta_i$.

As an aside, we note that if the tunneling paths were to cross, however, the commutation relations are modified to $T_{ij}T_{kl}+e^{2\pi i/g}T_{kl}T_{ij}=0$. It is hard to imagine a setup in which this occurs, but for such a scenario, we would need to take the even more exotic condition $\eta_1\eta_2=-e^{2\pi i/g}\eta_2\eta_1$ and cyclic permutations.

APPENDIX B: INSTANTON GAS BERRY'S PHASE CALCULATION

As we briefly sketched in Sec. III, when t is large, the interaction term dominates the action (2.8). If we treat k classically, it will be localized at one of the minima of this term. To find these minima, we need to diagonalize the 4×4 matrix $\Sigma_i(\eta_i S^+e^{-i\mathbf{R}^i\cdot\mathbf{k}}+\eta_i S^-e^{i\mathbf{R}^i\cdot\mathbf{k}})$. There are four solutions for each $\mathbf{k}$, corresponding to the four bands of a particle on a honeycomb lattice with π flux per plaquette. Physically, the fourfold multiplicity is due to the two charge states of the resonant level and the two states of the auxiliary two-state system (i.e., η) which keeps track of the statistics, while $\mathbf{k}$ represents the amount of charge that has been transferred between the leads. Diagonalizing $\Sigma_i(\eta_i S^+e^{-i\mathbf{R}^i\cdot\mathbf{k}}+\eta_i S^-e^{i\mathbf{R}^i\cdot\mathbf{k}})$ (we represent the η_i's by Pauli matrices τ_i), we find the four eigenvalues

$$\epsilon(k) = \pm[3 \pm \sqrt{9 - (3 + 2\cos k_y/\sqrt{2}) - 2\cos(k_x\sqrt{3/2g} + k_y/\sqrt{2g}) - 2\cos(k_x\sqrt{3/2g} - k_y/\sqrt{2g})}]^{1/2}. \quad \text{(B1)}$$

The minima of each of these bands form a honeycomb lattice with translation vectors $2\pi Q_i$, where the Q_i are given in Eq. (3.1).

We now consider the instanton gas expansion of the partition function, where the instantons are solutions of the classical equations of motion in which **k** tunnels between neighboring minima. The modulus of the amplitude for these tunneling events can be obtained in the standard way.[7] The phase can be obtained from the following Berry's phase argument. The eigenvector associated with the lowest energy band is determined by two spinors, i.e., it lies in the direct product space of the two two-dimensional spaces acted on by $S^{\pm}$ and η_i. As **k** tunnels from minimum to minimum, around a plaquette, these two spinors rotate. The phase aquired in a circuit around a plaquette is determined by the angles traced out by these spinors, $e^{i\phi_{\text{Berry}}} = e^{i(\theta_S + \theta_\eta)/2}$, where the factor of 1/2 follows from the fact that S and η are spin-1/2 degrees of freedom. Since, for any circuit, θ_S and θ_η must be multiples of 2π, the only possible nontrivial phase is π.

Let us consider the plaquette formed by the following six minima: $(0, \pm\pi\sqrt{2g}/3)$, $(\pi\sqrt{2g/3}, \pm 2\pi\sqrt{2g}/3)$, $(2\pi\sqrt{2g/3}, \pm\pi\sqrt{2g}/3)$. These six minima surround a maximum of the lowest band, at $(\pi\sqrt{2g/3}, 0)$, where the two lowest bands touch. The Berry phase will be the same for any loop that encloses $(\pi\sqrt{2g/3}, 0)$ precisely once since such loops can be adiabatically deformed into each other. The Berry phase is most simply computed for an infinitesimal loop enclosing $(\pi\sqrt{2g/3}, 0)$. For such a loop, we can approximate $\mathbf{k} = (\pi\sqrt{2g/3}, 0) + \mathbf{p}$, and

$$\begin{aligned}\sum_i (\eta_j \otimes S^+ e^{-i\mathbf{R}^i\cdot\mathbf{k}} + \eta_j \otimes S^- e^{i\mathbf{R}^i\cdot\mathbf{k}}) \approx & \left(\frac{1}{2}S_x - \frac{\sqrt{3}}{2}S_y\right)\otimes 1 \\ & + \left(\frac{\sqrt{3}}{2}S_x + \frac{1}{2}S_y\right)\otimes(\eta_z + \eta_x) - p_x\left(\frac{\sqrt{3}}{2}S_x + \frac{1}{2}S_y\right)\otimes 1 \\ & + \left(\frac{1}{2}S_x - \frac{\sqrt{3}}{2}S_y\right)\otimes\left[\left(\frac{\sqrt{3}}{2}p_y - \frac{1}{2}p_x\right)\eta_z \right. \\ & \left. - \left(\frac{\sqrt{3}}{2}p_y + \frac{1}{2}p_x\right)\eta_z\right]. \end{aligned} \quad \text{(B2)}$$

As **p** adiabatically traces out a loop enclosing $\mathbf{p} = 0$, the effective Zeeman field ''seen'' by η traces out a circle but the effective Zeeman field ''seen'' by **S** does not. In other words $\theta_\eta = 2\pi$ while $\theta_S = 0$. This can be made more transparent by projecting Eq. (B2) onto the two-dimensional subspace, which is degenerate at $\mathbf{p} = 0$. In an orthonormal basis of the two eigenvectors with degenerate eigenvalues at $\mathbf{p} = 0$, Eq. (B2) can be rewritten as

$$h(p_x, p_y)\tau + \text{const}, \quad \text{(B3)}$$

where τ are a set of Pauli matrices and $h(p_x, p_y)$ rotates by 2π as **p** adiabatically traces out a loop enclosing $\mathbf{p} = 0$.

Hence, a π phase is aquired in a circuit about a plaquette. Combining this with the magnitudes of the terms in the standard Coulomb gas expansion for the instanton gas,[7] we see that the dual theory to Eq. (2.8) is also a theory defined on a honeycomb lattice with π flux, namely, Eq. (3.2).

APPENDIX C: BOUNDARY CONDITIONS ON BOSONS

In this appendix, we summarize the conventions that we use for compactified bosons. Consider a single boson $\varphi(x, \tau)$ compactified on a circle of radius r. On a space of size l with periodic boundary conditions the action is

$$S_0 = \frac{1}{8\pi}\int_0^l dx \int_{-\infty}^{\infty} d\tau (\partial_\mu \varphi)(\partial^\mu \varphi),$$

where the functional integral is to be performed under the identification

$$\varphi(x, \tau) = \varphi(x, \tau) + 2\pi r = \varphi(x + l, \tau).$$

In the Hamiltonian formalism, the field operator is

$$\varphi(x) = \varphi_L(x) + \varphi_R(x),$$

where

$$\begin{aligned}\varphi_L(x) = & X_L + x\ \ P_L\frac{2\pi}{l} + i\sum_{n=1}^{\infty}\frac{1}{\sqrt{n}} \\ & \times[b_{L;n}e^{ixn2\pi/l} + b_{L;n}^\dagger e^{-ixn2\pi/l}], \\ \varphi_R(x) = & X_R - x\ \ P_R\frac{2\pi}{l} + i\sum_{n=1}^{\infty}\frac{1}{\sqrt{n}}[b_{R;n}e^{-ixn2\pi/l} \\ & + b_{R;n}^\dagger e^{ixn2\pi/l}]. \end{aligned} \quad \text{(C1)}$$

$b_{L;n}$ and $b_{R;n}$ are independent boson creation and annihilation operators, and

$$[X_L, P_L] = [X_R, P_R] = i\left(\frac{l}{2\pi}\right)$$

are two independent zero-mode coordinate and momentum operators. In these conventions, the two-point funtion of the boson is

$$\langle\varphi(x, \tau)\varphi(0,0)\rangle = -\ln(|z|^2), \quad (z = \tau + ix). \quad \text{(C2)}$$

The momentum operator, conjugate to the field $\varphi(x)$ is

$$\begin{aligned}\Pi(x) = (1/2)\frac{2\pi}{l}\Bigg\{ & (P_L + P_R) + \sum_{n=1}^{\infty}\sqrt{n}[b_{L;n}e^{ixn2\pi/l} \\ & + b_{L;n}^\dagger e^{-ixn2\pi/l}] + \sum_{n=1}^{\infty}\sqrt{n}[b_{R;n}e^{-ixn2\pi/l} \\ & + b_{R;n}^\dagger e^{ixn2\pi/l}]\Bigg\}. \end{aligned} \quad \text{(C3)}$$

The total momentum

$$\Pi=\int_0^l dx\Pi(x)=(1/2)[P_L+P_R]\frac{2\pi}{l}$$

is canonical conjugate to the total zero-mode coordinate $X\equiv X_L+X_R$. Since the latter is periodic with period $2\pi r$, the eigenvalues of ''dimensionless momentum'' P must be of the form

$$P=[P_L+P_R]=\frac{2n}{r},\quad n\in Z. \tag{C4}$$

On the other hand, periodicity under $x\to x+l$ gives, using Eq. (C1)

$$W\equiv P_L-P_R=rm,\quad m\in Z, \tag{C5}$$

where we denote this quantity by the *winding number* W. The two conditions (C4) and (C5) imply together that

$$P_L=\frac{n}{r}+\frac{1}{2}rm,\quad P_R=\frac{n}{r}-\frac{1}{2}rm. \tag{C6}$$

The (normal ordered) Hamiltonian is

$$H=\frac{2\pi}{l}\left[L_{0;L}+L_{0;R}-\frac{1}{12}\right], \tag{C7}$$

where

$$\begin{aligned}L_{0;L}&=\frac{1}{2}P_L^2+\sum_{n=1}^{\infty} n\ \ b_{L;n}^{\dagger}b_{L;n},\\ L_{0;R}&=\frac{1}{2}P_R^2+\sum_{n=1}^{\infty} n\ \ b_{R;n}^{\dagger}b_{R;n}.\end{aligned} \tag{C8}$$

Note that

$$\frac{1}{2}[P_L^2+P_R^2]=[(n/r)^2+(rm/2)^2]$$

gives the total scaling dimension.

The (imaginary time evolved) Heisenberg operators are obtained from the expressions in Eqs. (C1) and (C3) by $ix\to z=\tau+ix$ for left movers, and by $ix\to z^*=\tau-ix$ for right movers.

Of interest is also the *dual* boson field,

$$\tilde{\varphi}(x)=\varphi_L(x)-\varphi_R(x). \tag{C9}$$

We see that the automorphism of the canonical commutation relations

$$\begin{aligned}&X_R\to -X_R,\quad P_R\to -P_R,\quad b_{R,n}\to -b_{R,n},\\ &b_{R,n}^{\dagger}\to -b_{R,n}^{\dagger},\qquad r\to\tilde{r}\equiv 2/r\end{aligned} \tag{C10}$$

(all left-movers unchanged) maps the boson field $\varphi(x)$ into its dual $\tilde{\varphi}(x)$. The dual field then satisfies the periodicity condition $\tilde{\varphi}(x)=\tilde{\varphi}(x)+2\pi\tilde{r}$ where $\tilde{r}$ is the *dual* compactification radius. Note that, most importantly, the duality automorphism exchanges the lattice of momenta P (C4) with the lattice of winding numbers W (C5).

1. Boundary conditions

Next, consider the compactified boson in *semi-infinite* space, $0<x<\infty$. First, we impose a Neumann boundary condition (bc) on the boson field at $x=0$,

$$\partial_x\varphi(x,\tau)\to 0\quad (x\to 0) \tag{C11}$$

For the purpose of analyzing this bc it is convenient to view the imaginary time coordinate as a spatial coordinate $\tilde{x}\equiv\tau$, and the original spatial coordinate x as (imaginary) time, $\tilde{\tau}\equiv -x$. The new complex coordinates, are just rotated by 90° with respect to the original ones, $\tilde{z}\equiv\tilde{\tau}+i\tilde{x}=iz$, $\tilde{z}^*\equiv\tilde{\tau}-i\tilde{x}=(-i)z^*$ (this may be viewed as a trivial conformal transformation). We may quantize the system as before, but now on equal $\tilde{\tau}$ slizes. The ''spatial'' coordinate $\tilde{x}=\tau$ is now compact, corresponding to the original system being at finite inverse temperature $\beta<\infty$. The Heisenberg operators in this quantization become

$$\begin{aligned}\varphi_L(\tilde{x},\tilde{\tau})&=X_L-i(\tilde{\tau}+i\tilde{x})\ \ P_L\frac{2\pi}{\beta}+i\sum_{n=1}^{\infty}\frac{1}{\sqrt{n}}[b_{L;n}e^{(\tilde{\tau}+i\tilde{x})n2\pi/\beta}\\ &\quad+b_{L;n}^{\dagger}e^{-(\tilde{\tau}+i\tilde{x})n2\pi/\beta}],\\ \varphi_R(\tilde{x},\tilde{\tau})&=X_R-i(\tilde{\tau}-i\tilde{x})\ \ P_R\frac{2\pi}{\beta}+i\sum_{n=1}^{\infty}\frac{1}{\sqrt{n}}[b_{R;n}e^{(\tilde{\tau}-i\tilde{x})n2\pi/\beta}\\ &\quad+b_{R;n}^{\dagger}e^{-(\tilde{\tau}-i\tilde{x})n2\pi/\beta}].\end{aligned} \tag{C12}$$

Note that the currents associated with translations of the two chiral bosons are the left/right momenta

$$J_L=i\partial_{\tilde{z}}\varphi_L=P_L\frac{2\pi}{\beta}+\text{oscillators},$$

$$J_R=i\partial_{\tilde{z}}\varphi_R=P_R\frac{2\pi}{\beta}+\text{oscillators}$$

The Neumann bc now becomes an identity for Heisenberg operators, acting on a boundary state $|N\rangle$:

$$\partial_{\tilde{\tau}}\hat{\varphi}(\tilde{x},\tilde{\tau})|N\rangle\to 0\qquad(\tilde{\tau}\to 0). \tag{C13}$$

Integrating this equation over $\tilde{x}$ implies in particular that the total momentum operator $\hat{P}=\hat{P}_L+\hat{P}_R$ annihilates the Neumann boundary state but the winding number $W=P_L-P_R=2P_L$ may take on any value on the lattice specified in Eq. (C5). (This is clear since the Neuman bc only constrains the derivative of the field.) Specifically, the only momentum states which the Neumann boundary condition supports are those with $n=0$ in Eq. (C6). Unfolding the semi-infinite system with a boundary thus gives an infinite chiral system of bosons with only those momenta allowed.

Next consider the Dirichlet boundary condition

$$\varphi(x,\tau)\to 0\quad (x\to 0).$$

After 90° rotation, this becomes an identity for Heisenberg operators, acting on a ''Dirichlet'' boundary state $|D\rangle$:

$$\hat{\varphi}(\tilde{x},\tilde{\tau})|D\rangle \to 0 \quad (\tilde{\tau}\to 0).$$

This implies that the total winding-number operator, $\hat{W}=\hat{P}_L-\hat{P}_R$ annihilates the Dirichlet boundary state, but the total momentum $P=2P_L$ lies on the lattice specified in Eq. (C4). (The winding number is seen to be zero also because of the operator identity $X_L+X_R=0$, which follows from the Dirichlet bc.) Specifically, the only momentum states, which the Dirichlet boundary condition supports are those with $m=0$ in Eq. (C6). Unfolding the semi-infinite systems gives thus an infinite chiral system with only those momenta allowed.

2. Duality and boundary conditions

It immediately follows from the discussion above that the duality operation exchanges Dirichlet and Neuman boundary conditions. In other words, a Dirichlet bc on the field φ is a Neuman bc on the dual field $\tilde{\varphi}$ and vice versa.

APPENDIX D: TRANSFORMATION OF THE CONDUCTANCE UNDER DUALITY

The conductance can be obtained from the two-point function

$$\langle J^3(\tau_1,x_1)J^3(\tau_2,x_2)\rangle,$$

where

$$J^3(\tau,x)=J_L^3+J_R^3$$

and $J_{R,L}^3$ is proportional to $\partial\varphi_{R,L}^3$. At the location of the point contact, we obtain four terms, which are pairwise equal,

$$\langle J^3(\tau_1,0)J^3(\tau_2,0)\rangle = 2(1+A)/(\tau_1-\tau_2)^2,$$

where A is the amplitude of the right-left current-current correlator,

$$\langle J_L^3(\tau_1,x_1)J_R^3(\tau_2,x_2)\rangle = A/(z_1-z_2^*)^2$$

($z_i=\tau_i+ix_i$), and

$$\langle J_L^3(\tau_1,x_1)J_L^3(\tau_2,x_2)\rangle = 1/z_{12}^2$$

(similar for right movers).

The conductance can be written as

$$G=g(1-A).$$

This we may rewrite as

$$G=2g[1/2-A/2]=2g[1-(1+A)/2].$$

On the other hand, we have

$$(1+A)/2=\frac{|\omega|}{2\pi}\langle\varphi^3(x=0,\omega)\varphi^3(x=0,\omega)\rangle,$$

where ω is a real frequency, and $\varphi^3=\varphi_L^3+\varphi_R^3$. Under duality, $A\to -A$, which may also be written as

$$\frac{|\omega|}{2\pi}\langle\varphi^3(x=0,\omega)\varphi^3(x=0,\omega)\rangle \to \left[1-\frac{|\omega|}{2\pi}\langle\tilde{\varphi}^3(x=0,\omega)\tilde{\varphi}^3(x=0,\omega)\rangle\right].$$

Clearly, for Neumann boundary conditions, we have have $A=1$, yielding $G=0$. For Dirichlet boundary condition on φ^3 (as opposed to Dirichlet boundary conditions on k_x, k_y), $A=-1$, yielding, $G=2g$.

Since we will not impose boundary conditions on the fields φ^j directly, we rewrite the conductance in terms of the fields defined in Eq. (2.7), giving

$$G=\frac{4g}{3}\left[1-\frac{|\omega|}{2\pi}\langle k_x k_x\rangle_\omega\right].$$

Under the duality transformation, $k_x\to\tilde{k}_x=r_x$, we have

$$G\to\tilde{G}=\frac{4\tilde{g}}{3}\frac{|\omega|}{2\pi}\langle r_x r_x\rangle_\omega$$

At the self-dual point, $g=\tilde{g}=\sqrt{3}$, and

$$[1-(|\omega|/2\pi)\langle k_x k_x\rangle_\omega]=(|\omega|/2\pi)\langle r_x r_x\rangle_\omega=1/2.$$

[1] See, e.g., I. Affleck and A.W.W. Ludwig, Nucl. Phys. B **360**, 641 (1991); **428**, 545 (1994); A.W.W. Ludwig, Int. J. Mod. Phys. B **8**, 347 (1994); I. Affleck, Acta Phys. Pol. B **26**, 1869 (1995); S. Eggert and I. Affleck, Phys. Rev. B **46**, 10 866 (1992).

[2] P.B. Wiegman and A.M. Tsvelik, Pis'ma Zh. Éksp. Teor. Fiz. **38** 489 (1983) [JETP Lett. **38**, 591 (1983); Adv. Phys. **32**, 543 (1983); N. Andrei, K. Furuya, and J. Lowenstein, Rev. Mod. Phys. **55**, 331 (1983).

[3] P. Fendley, A.W.W. Ludwig, and H. Saleur, Phys. Rev. Lett. **74**, 3005 (1995); Phys. Rev. B **52**, 8934 (1995).

[4] C.L. Kane and M.P.A. Fisher, Phys. Rev. Lett. **68**, 1221 (1992); Phys. Rev. B **46**, 15 233 (1992).

[5] V.J. Emery and S. Kivelson, Phys. Rev. B **46**, 10 812 (1992).

[6] H. Yi and C.L. Kane, cond-mat/9602099 (unpublished).

[7] A. Schmid, Phys. Rev. Lett. **51**, 1506 (1983); M.P.A. Fisher and W. Zwerger, Phys. Rev. B **32**, 6190 (1985).

[8] *Bosonization*, edited by M. Stone (World Scientific, Singapore, 1994).

[9] E. Wong and I. Affleck, Nucl. Phys. B **417**, 403 (1994).

[10] I. Affleck and A.W.W. Ludwig, J. Phys. A **27**, 5375 (1994).

[11] See, for example, P. Ginsparg, in *Fields, Strings, and Critical Phenomena*, edited by E. Brezin and J. Zinn-Justin, (North-Holland, Amsterdam, 1990).

[12] M.P.A. Fisher and L. Glazman, cond-mat/9610037 (unpublished).

[13] A.M. Sengupta and Y.B. Kim, cond-mat/9602100 (unpublished).

[14] C. de C. Chamon and E. Fradkin, Phys. Rev. B **56**, 2012 (1997); N.P. Sandler, C. de C. Chamon, and E. Fradkin, cond-mat/9704189 (unpublished).

[15] For recent discussions of the Callan-Rubakov effect, see, for example, J. Polchinski, Nucl. Phys. B **242**, 345 (1984); I. Affleck and J. Sagi, *ibid.* **417**, 374 (1994).